Journal of Materials Chemistry B

ROYAL SOCIETY OF CHEMISTRY

PAPER

View Article Online
View Journal | View Issue

Cite this: J. Mater. Chem. B, 2023, 11, 7435

Development of cationic peptide-based hydrogels loaded with iopamidol for CEST-MRI detection†

Enza Di Gregorio, ‡[a] Elisabetta Rosa,‡[b] Giuseppe Ferrauto,[a] Carlo Diaferia,[b] Enrico Gallo,[c] Antonella Accardo *[b] and Enzo Terreno *[a]

Received 30th January 2023,
Accepted 30th June 2023

DOI: 10.1039/d3tb00187c

rsc.li/materials-b

Peptide-based hydrogels have been recently investigated as materials for biomedical applications like tissue engineering and delivery of drugs and imaging agents. Among the synthetic peptide hydrogelators, the cationic hexapeptides Ac-K1 and Ac-K2 were proposed as scaffolds for bioprinting applications. Here, we report the formulation of Ac-K1 and Ac-K2 hydrogels loaded with iopamidol, an iodinated contrast agent clinically approved for X-ray computed tomography, and more recently identified as an efficient CEST-MRI probe. Iopamidol-loaded hydrogels were soft, injectable and non-toxic both *in vitro* (on three tumor cell lines: GL261, TS/A and 3T3-NIH) and *in vivo* (in Balb/c mice inoculated with TS/A breast cancer cells). The *in vitro* CEST-MRI study evidenced the typical features of the CEST pattern of iopamidol, with a CEST contrast higher than 50%. Due to their injectability and good ability to retain the contrast agent, the herein investigated systems can be considered as promising candidates for the development of smart MRI detectable hydrogels.

Introduction

Magnetic resonance imaging (MRI) is a powerful diagnostic technique commonly used in radiology to image the interior of the human body. In the last few years, the wide use of gadolinium(III) based paramagnetic complexes as MRI contrast agents (CAs) in clinical practice has been questioned due to the evidence that a certain number of free Gd ions may be retained and accumulated in body sites of patients receiving multiple doses of CAs.[1] Even for this reason, research in this field has been moving towards alternative solutions to image the human anatomy and to obtain functional information on the disease onset and development. In this context, new methods and techniques are emerging. Among them, the Chemical Exchange Saturation Transfer (CEST) MRI contrast is a very interesting option that implies the presence of endogenous or exogenous molecules containing exchangeable spins. When such spins are selectively saturated by the application of an appropriate radio-frequency pulse, the saturation is transferred, through a chemical exchange, to the bulk spins with the consequent decrease of their MRI detectable signal. This allows indirectly detecting chemicals at low concentrations by observing their effect on the much more abundant bulk spins.[2] Among the free-metal exogenous CEST probes, iodinated CT agents represent a valuable option for two main reasons: (i) they have exchangeable protons with the appropriate exchange regime for CEST detection and (ii) they are already approved for clinical use with an excellent safety profile, thus ensuring a high clinical translatability potential.[3] Iopamidol (Fig. 1) has been the first iodinated CT agent considered for CEST-MRI,[4] and it has also been demonstrated to act as an excellent *in vivo* pH reporter.[5–7]

CEST agents have been investigated for many clinically relevant applications, including the possibility of labeling hydrogels (HGs), thus making them detectable by MRI. Hydrogels are supramolecular network structures able to retain a high amount of water and mainly studied as platforms to encapsulate and release bioactive compounds[8,9] or as scaffolds for supporting living cells.[10]

Two strategies have been adopted to make hydrogels detectable by CEST-MRI: (i) using hydrogel building blocks bearing exchangeable spins,[11–16] and/or (ii) loading hydrogels with a CEST agent.[17]

HGs can be obtained starting from different building blocks,[18] among which peptides have been occupying a central position because of their chemical versatility and low cost.[19,20]

[a] Molecular and Preclinical Imaging Center, Department of Molecular Biotechnology and Health Sciences, University of Turin, Via Nizza 52, Turin, Italy. E-mail: enzo.terreno@unito.it
[b] Department of Pharmacy and Interuniversity Research Centre on Bioactive Peptides (CIRPeB) "Carlo Pedone", University of Naples "Federico II", Via D. Montesano 49, Naples 80131, Italy
[c] IRCCS Synlab SDN, Via Gianturco 113, Naples, 80143, Italy

† Electronic supplementary information (ESI) available: Supplementary experimental data: chemicals, peptide solid phase synthesis and characterization, cell cultures, cell viability: MTT assay; supplementary references; supplementary figures: chemical structures and RP-HPLC chromatograms of Ac-K1 and Ac-K2; oscillation strain and frequency sweep test for hydrogels; Z- and ST%-spectra of Ac-K1 hydrogels loaded with iopamidol at acidic pH. See DOI: https://doi.org/10.1039/d3tb00187c

‡ These authors have contributed equally.

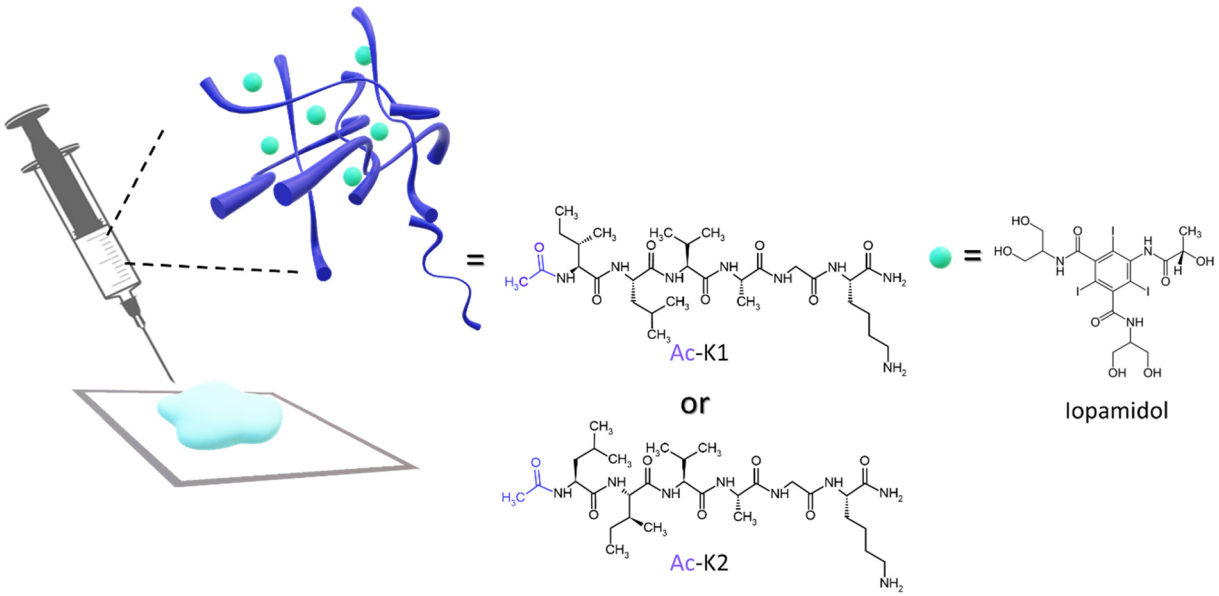

Fig. 1 Chemical structures of the cationic hexapeptides and iopamidol, used for the formulation of the hydrogels.

In fact, the mutual intervention on the primary peptide sequence can allow changing the chemical and the physical properties of the final macroscopic materials, thus allowing their utilization for many different biomedical purposes.[21,22] Regarding the delivery of active pharmaceutical ingredients, the introduction of hydrophilic residues instead of hydrophobic ones leads to the encapsulation of water-soluble molecules, or *vice-versa*. Moreover, also the electrostatic interactions between the components can modulate the overall properties of the hydrogels. In the literature, some self-assembling cationic peptide sequences have been proposed for wound healing and bio-ink applications.[23] Among them, we selected two hexapeptides, namely Ac-K1 and Ac-K2 (Fig. 1), characterized by five aliphatic amino acids (including isoleucine, leucine, valine, alanine, and glycine) followed by a Lys at the C-terminus, which was amidated to avoid the formation of zwitterions.[23] These two sequences were found to be able to form a gel with high stiffness under physiological conditions, which is an important requisite to design a delivery system with proper drug retention. Due to their cationic nature, they were also utilized as vehicles to increase the performance of anionic Gd-complex contrast agents.[24] In this work, iopamidol was loaded into Ac-K1/Ac-K2 HGs as a CEST-MRI reporter for monitoring drug loading and release and potentially acting as a pH sensor of the hydrogel scaffold. The hydrogels were characterized in terms of their physicochemical properties, biocompatibility, and imaging performances, providing an *in vivo* proof-of-concept of their potential applications.

Results and discussion

HG preparation and mechanical characterization

Ac-K1 and Ac-K2 are two cationic hexapeptides containing five aliphatic residues and a lysine at their C-terminus. Moreover, both the peptides are amidated and acetylated at the C- and the N-terminus, respectively (Fig. 1 and Fig. S1 and S2, ESI†). The acetyl (Ac-) group was a determining factor in influencing the mechanical properties of the hydrogels. Indeed, we previously observed that the replacement of the acetyl moiety with the fluorenyl (Fmoc-) one caused a certain decrease of the hydrogel rigidity.[25] It is expected that the slight difference between the two peptides in terms of hydrogel stiffness can be attributed to the inversion of isoleucine and leucine amino acids in the primary sequence. Due to the presence of the lysine residue, gelation of Ac-K1 and Ac-K2, as well as the corresponding Fmoc-analogues, is prompted by the addition of a few microliters of phosphate buffer solution to the limpid peptide solution at a concentration of 2 wt%. Ac-K1 and Ac-K2 hydrogels were used as matrices for the encapsulation of iopamidol (Fig. 1), an iodinated clinically approved contrast agent for X-ray computed tomography (marketed as Isovue®), herein used as a representative example of a small-size and MRI detectable probe. Indeed, iopamidol has been widely reported to be a very efficient CEST-MRI contrast agent, containing three pools of exchangeable protons resonating at 1.5 ppm (hydroxyl protons), 4.2 ppm (amide protons of benzamido side chains), and 5.5 ppm (amide protons of the 2-hydroxypropanamido side chain) from bulk water proton signals.[26] The first signal displays a pH-independent CEST contrast (in the pathophysiological pH window), whereas the other two signals show a pH-dependent CEST response, which has been successfully used for *in vivo* extracellular/extravascular pH mapping.[27] Iopamidol-loaded Ac-K1 and Ac-K2 hydrogels were prepared by dissolving the peptide powder (2 wt%) in a 223 mM aqueous solution of iopamidol (buffered at physiological pH by PBS). The addition of the saline buffer allows reduction of the electrostatic repulsion between the lysine chains and triggers gel formation. According to its chemical structure and its very high-water solubility ($\sim$120 mg mL^{-1}),[28] we suppose that iopamidol is

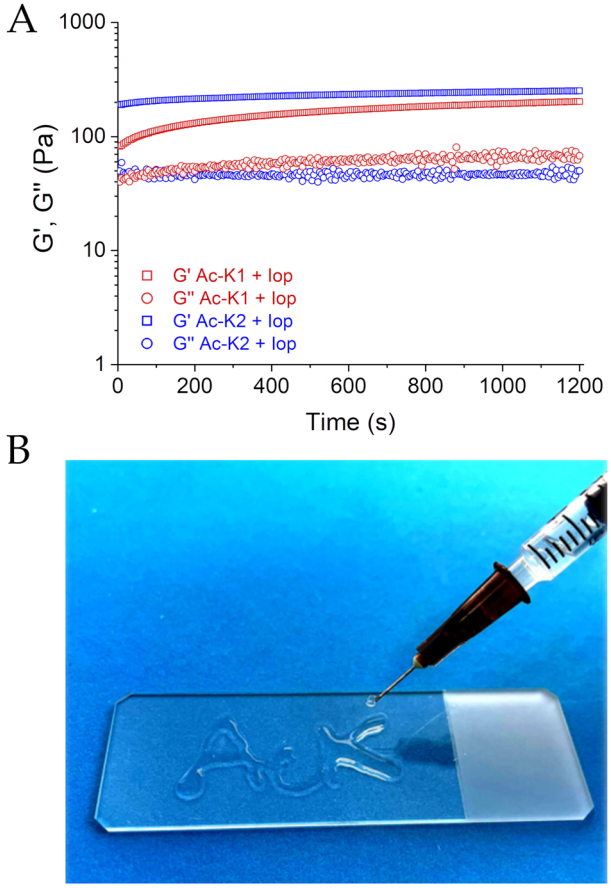

Fig. 2 (A) Rheological characterization of Ac-K1 and Ac-K2 loaded with iopamidol: time sweep rheological analysis of hydrogels reported as storage modulus (G') and loss modulus (G''). (B) Test of syringability on Ac-K1.

mainly located in the hydrophilic interface of the hydrogel, where hydrogen bonds can occur between iopamidol and the bulk solvent. However, we cannot exclude that iopamidol is also partially located in the hydrophobic spine of the fibers that compose the hydrogel. The effect of the physical entrapment of iopamidol in the hydrogel in terms of mechanical response was evaluated. The viscoelastic features of the resulting peptide based HGs have been evaluated by oscillatory rheological studies. The results, reported as G' (storage modulus) and G'' (Loss modulus), are plotted in Fig. 2A. Two dynamic tests were carried out: an oscillation strain sweep (at a frequency of 1.0 Hz) and a frequency sweep (at 0.1% strain) (Fig. S3, ESI†). The linear viscoelastic region (LVE region) for both the systems was in the 0.01–2.0% strain range. The LVE region indicates the oscillation range in which the rheological tests can be carried out without destroying the viscoelastic nature of the samples. The time sweeps for both iopamidol containing peptide hydrogels, acquired for 20 minutes at a frequency of 1.0 Hz and at 0.1% strain, are shown in Fig. S3 (ESI†).

The tan δ (G'/G'') values for both matrices exceeded 1 (tan δ Ac-K1 = 3.03 and tan δ Ac-K2 = 5.02), thus confirming the hydrogel state. The K2-sequence, possessing a larger tan δ value, displayed a more pronounced viscoelastic behavior, as also verified comparing the G' values (G' = 251 Pa/G'' = 50 Pa and G' = 203 Pa/G'' = 67 Pa for Ac-K2 and Ac-K1, respectively). The obtained G' values are indicative of the soft nature of these matrices and suggest good suitability for *in vivo* applications, considering the requirements of injectable preparations. Additionally, the iopamidol entrapment caused a decrease in the mechanical response of matrices with respect to the corresponding empty systems, especially in Ac-K2-based hydrogels (G' values of 306 Pa and 2677 Pa for pure Ac-K1 and Ac-K2, respectively). The decrease in rigidity could be ascribed to a modification in the non-covalent interactions of fiber entanglement with a consequent reduction in physical and reversible cross-networking. Injectability through a 27-G syringe on a plastic support was evaluated for Ac-K1 and Ac-K2 hydrogels. After being extruded through the needle, the metastable solution of both peptide derivatives turned again into a hydrogel in a few minutes, thus demonstrating their self-healing properties (as an example in Fig. 2B, the result of the experiment for Ac-K1 is reported). The reconstruction of both hydrogels was found to be fast. After reconstruction, both the hydrogels exhibited the same rheological and swelling properties of the native samples, thus confirming their state of gel (data not shown).

In vitro MRI-CEST study

Fig. 3 shows *Z*- and ST%-spectra measured at room temperature and physiological pH for Ac-K1/Ac-K2 hydrogels loaded with iopamidol. Data for free iopamidol and empty Ac-K1 hydrogels, measured in the same experimental conditions, are displayed as the reference. Iopamidol-loaded Ac-K1 and Ac-K2 hydrogels replicate the typical features of the CEST pattern of iopamidol at pH 7.4, with a predominant ST effect at 4.2 ppm, whereas Ac-K1 empty hydrogel (and Ac-K2 as well) did not display any significant CEST contrast. The absence of mobile protons in the hydrogels was also confirmed by the much narrower signal of the bulk water in the corresponding *Z*-spectrum. Both peptide hydrogels showed a very similar CEST performance, with a very slight superior effect (*ca.* 5–7%) measured for Ac-K1. Hydrogels prepared with Ac-K1 are bit softer and maybe this property leads to a small change in the exchange rate of the mobile protons of iopamidol embedded in the gel. Since the observed CEST contrast was slightly higher for Ac-K1 preparation, this formulation was selected for the following studies.

When loaded into the hydrogels, the CEST profile of iopamidol displayed small changes in the ST contrast likely attributable to variations in the exchange rate of the mobile protons that result in a reduction of the CEST contrast at 1.5 ppm and an overall broadening of all the CEST signals. CEST experiments on the iopamidol-loaded Ac-K1 HG were also performed at pH 6.8 (Fig. S4, ESI†), which confirmed the well-established higher pH responsiveness of the CEST at 4.2 ppm,[26] and the appearance of a pH dependence for the signal at 1.5 ppm for the agent loaded in the HG.

In vitro release study

The *in vitro* release of iopamidol from the Ac-K1 hydrogel was studied over time. For this purpose, the hydrogel was put in

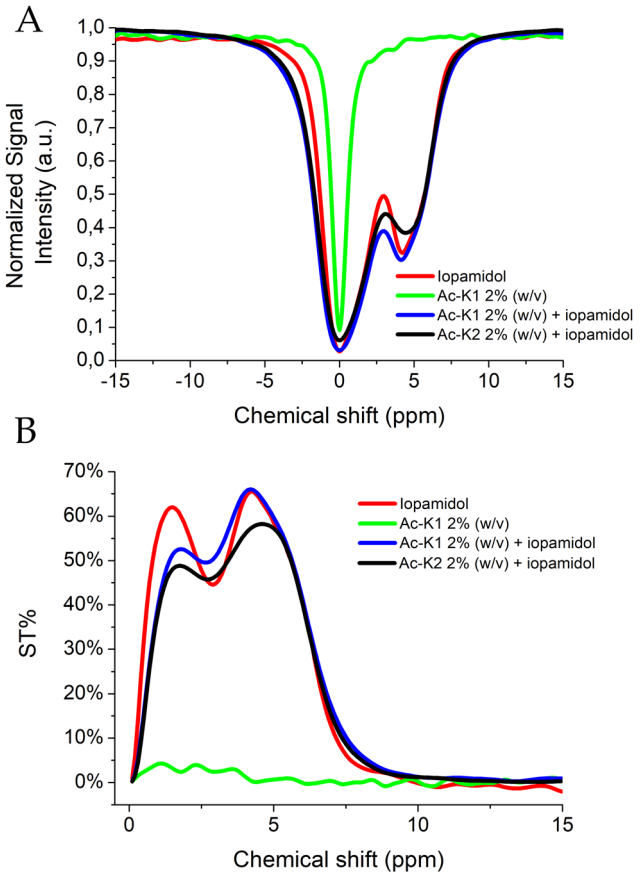

Fig. 3 *Z*- (A) and ST%- (B) spectra of iopamidol (223 mM) loaded hydrogels (2% wt) at physiological pH and room temperature. Spectra of free iopamidol and Ac-K1 empty hydrogel measured in the same experimental conditions are also reported for comparison.

contact with PBS and subjected to repeated sampling of the supernatant (up to 3 days), which was replaced each time with fresh PBS solution. UV-vis measurements carried out at λ = 240 nm have been used to quantify the amount of the agent in the drawn fraction. The iopamidol concentration (reported in Fig. 4) was calculated, for each point, by adding the amount released at the time considered to the amount previously moved away. The maximum release (*ca.* 11%) was reached at *ca.* 24 h from the hydrogel preparation. The observation that the maximum release observed was much lower than the full one is indicative of a very stable loading. This result also suggests that iopamidol is likely entrapped in the hydrogel in two chemical environments with one fraction being more loosely held and more quickly released, and the other one more stably entrapped, probably through the hydrogen bonds, and still retained after 3 days. The release profile of iopamidol from the Ac-K1 hydrogel suggests that this peptide matrix could be a potential scaffold for the topic administration of bioactive compounds and for monitoring their release *in vivo*.

Cytotoxicity study

The *in vitro* biocompatibility of Ac-K1 and Ac-K2 empty hydrogels was assessed by measuring the viability by MTT assay on

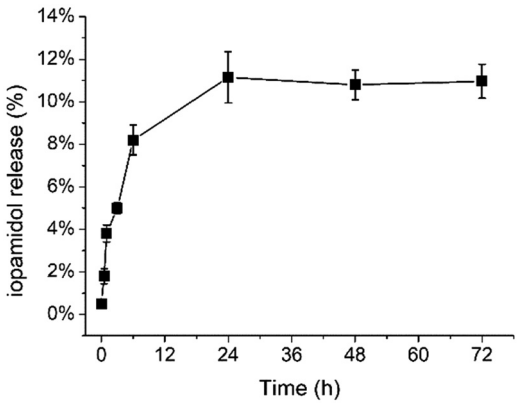

Fig. 4 *In vitro* release of iopamidol from the Ac-K1 hydrogel. For the experimental conditions and procedure, please refer to the Experimental section.

three different cell lines: (i) GL261 (murine glioma), (ii) TS/A (murine breast carcinoma), and iii) 3T3-NIH (murine fibroblasts). Cells were pre-incubated for 24 h with the hydrogel to verify cell viability. As reported in Fig. 5 for Ac-K1, the hydrogel did not show any evident cytotoxicity, with a very small effect (viability 90%) for TS/A cells. Similar results were obtained for the Ac-K2 system.

This result agrees with previous studies reported for similar peptide based HGs.[23–25]

In vivo imaging of Ac-K1 hydrogels by CEST-MRI

Based on the promising preliminary *in vitro* results, an *in vivo* proof of concept for the feasibility of using the iopamidol-loaded Ac-K1 hydrogel was pursued by intratumor injection of the scaffold into Balb/c mice (n = 3) subcutaneously inoculated with TS/A breast cancer cells. Animals were included in the study when the tumours reached a volume of *ca.* 400 ± 50 mm^3. Then, *ca.* 50 μL of Ac-K1-iopamidol hydrogel was injected into the tumour mass. MRI scans were performed before and after the injection of the hydrogel. MRI-CEST experiments (carried out up to 24 hours post injection of the hydrogel) were used to monitor the fate of the loaded iopamidol. Fig. 6A shows T_{2w}- and CEST-MR images acquired after saturation at 4.2 and 5.5 ppm of a

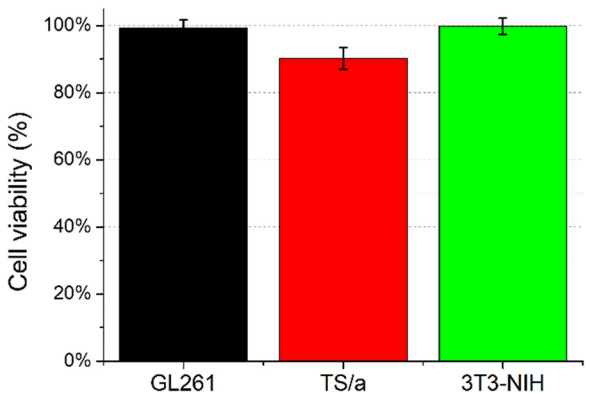

Fig. 5 Cell viability assessed by MTT assay for GL261, TS/A, and 3T3-NIH cells incubated for 24 hours in the presence of culture media conditioned with the Ac-K1 hydrogel.

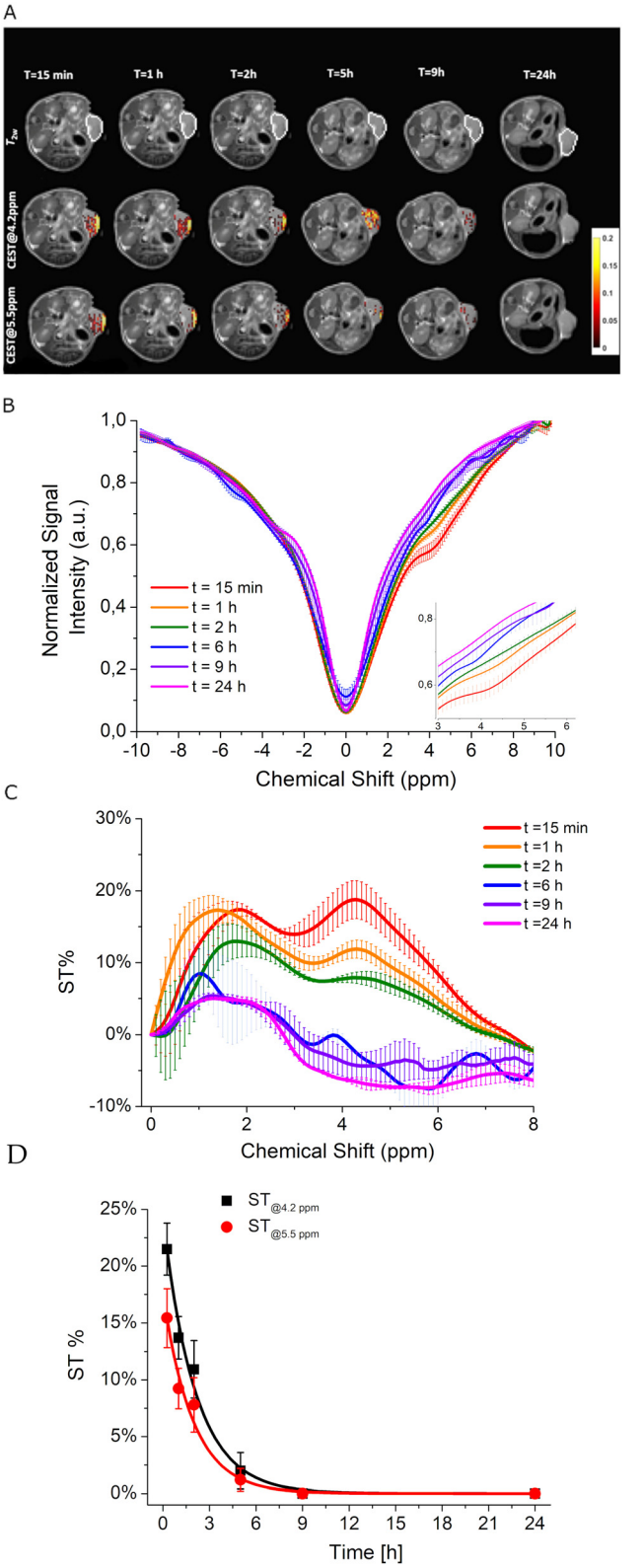

Fig. 6 (A) T_{2w}, $CEST_{@4.2ppm}$ and $CEST_{@5.5ppm}$ MR images of a representative mouse upon intratumor injection of iopamidol-loaded Ac-K1 hydrogel at different time points (from 15 min to 24 hours). Corresponding (B) *Z*- and (C) ST% spectra averaged out on three mice. (D) Time evolution of the intratumor ST% values.

representative mouse. MR images were acquired at different time points post-injection (from 15 min to 24 hours). Fig. S5 and S6 (ESI†) show T_{2w}- and CEST-MR images of the other two mice.

The time evolution of the ST profiles of the tumour averaged in the three mice (Fig. 6B) displayed a quite rapid decrease in CEST contrast with a return to the initial basal level reached 9 hours post injection (Fig. 6C). The data fit well with first-order kinetics with an intratumor residence half-time of iopamidol of *ca.* 1.4 h, demonstrating a much faster release of the agent in the tumour microenvironment than in the *in vitro* experiments.

Experimental

Formulation of iopamidol-loaded hydrogels

Each peptide was dissolved in 300 μL of a water solution of 260 mmol L^{-1} of iopamidol under sonication. The concentration of the peptide in the resulting solution was 2 wt%. Then, 50 μL of phosphate buffer (100 mmol L^{-1} phosphates) was added, and the mixture was vortexed to allow gel formation (final concentration of peptide 2 wt%, final concentration of iopamidol 223 mmol L^{-1}).

Rheological studies

Rheological characterization of the iopamidol-loaded hydrogels was performed using a rotationally controlled stress rheometer (Malvern Kinexus) with a 15 mm flat-plate geometry (PU20:PL61). The measurements were carried out on 400 μL of freshly prepared samples at a concentration of 2 wt%. Each experiment was performed at 25 °C in a humidity chamber and a gap of 1 mm. Preliminary dynamic rheological tests were carried out to identify the regime of linear viscoelasticity. The viscous elastic region was determined by the oscillatory frequency (0.1–100 Hz) and the strain sweep (0.01–100%). A time-sweep oscillatory evaluation test (using a constant 0.1% strain and 1 Hz frequency) was then performed for 20 minutes. Results are reported in pascals (Pa) as shear storage or elastic modulus (G') and shear loss or viscous modulus (G'').

Iopamidol release from hydrogels

350 μL of Ac-K1 HG was prepared, as described above, in a 1.5 mL Eppendorf tube. Then, 700 μL of 10 mmol L^{-1} of PBS was added on top of the gel. At well-defined time points (30 min, 1 h, 3 h, 6 h, 9 h, 12 h, 24 h, 36 h, 48 h, 60 h and 72 h), 350 μL of the supernatant on top of the HG was removed and replaced with an equal amount of fresh PBS. The amount of iopamidol in each fraction was analyzed through UV-vis spectroscopy (λ_{abs} = 240 nm). The release profile was obtained by plotting the amount of iopamidol released over time. The experiment was repeated twice, and the data are presented as mean value ± standard deviation.

Animal models

In vivo experiments were carried out using 8–10 week-old female Balb/C mice (Charles River Laboratories, Calco, Italy)

bred at the Department of Molecular Biotechnology and Health Sciences, University of Turin, Italy. Mice were kept in standard housing (12 h light/dark cycle) with rodent chow and water available *ad libitum*. The experiments were performed according to the Amsterdam Protocol on Animal Protection and in conformity with institutional guidelines that are in compliance with national laws (D.L.vo 116/92, D.L.vo 26/2014 and following additions) and international laws and policies (2010/63/EU, EEC Council Directive 86/609, OJL 358, Dec 1987, NIH Guide for the Care and Use of Laboratory Animals, U.S. National Research Council, 1996).

For the tumor model preparation, *ca.* 3×10^5 TS/A breast cancer cells were suspended in 0.1 mL of PBS and subcutaneously injected in the flank of 8–10 week-old female mice ($n = 3$ for each tested group), a small number in agreement with 3Rs principles for use of animals, considering that only a proof of concept for the *in vivo* feasibility of the system was proposed. For the experiments, mice were anesthetized by intramuscular injection of tiletamine/zolazepam (Zoletil 100; Virbac, Milan, Italy) 20 mg kg^{-1} plus xylazine (Rompun; Bayer, Milan, Italy) 5 mg kg^{-1} using a 27-G syringe. Animals were monitored weekly for changes in tumor size using calipers. Experiments were carried out 2 weeks after tumor cell implantation when the mean tumour volume is *ca.* 400 ± 50 mm^3. About 50 μL of each hydrogel was implanted intratumorally using a 27-G syringe. CEST-MR images were recorded as reported below.

At the end of the experiments, mice were sacrificed by cervical dislocation in agreement with ethical guidelines.

MRI and data analysis

MR images of phantoms and mice were acquired at 7 T using a Bruker Avance 300 spectrometer equipped with a Micro 2.5 microimaging probe (room temperature, *ca.* 21 °C). T_{2w} images were acquired using a standard T_{2w} RARE (Rapid Acquisition with Refocused Echoes) sequence with the following parameters (Repetition Time (TR) 5000 ms, Echo Time (TE) 5.5 ms, RARE factor 24, Number of averages 4, 128×128 isotropic acquisition matrix with a FOV of 30 mm and a slice thickness of 1 mm). *Z*-spectra were acquired by using a typical RARE spin–echo sequence with the following parameters: TE 3 ms, TR 5 s, RARE factor 32, number of averages 1. An isotropic 64×64 acquisition matrix with a FOV of 30 mm and a slice thickness of 1 mm was used. The whole sequence was preceded by a saturation scheme consisting of a continuous rectangular wave pulse 2 s with a radiofrequency intensity of 3 μT. A frequency-offset range of ± 20 ppm was investigated.

The *Z*-spectra were interpolated by smoothing splines to identify the zero offset on a pixel-by-pixel basis of the bulk water and then to assess the correct ST% value over the entire range of frequency offsets investigated. A custom-made analysis algorithm, compiled in Matlab (Mathworks Inc., Natick, MA), was used. The CEST effect is calculated by using the following formula:

$$ST\% = (1 - M_S/M_0) \times 100$$

where M_S is the intensity of the bulk water NMR signal after the on-resonance saturation on the mobile proton pool of iopamidol ($\Delta\omega$), and M_0 is the intensity of the bulk water NMR signal after the contralateral frequency ($-\Delta\omega$). The resonance of the bulk water protons was set to 0.

Conclusions

Compared to polymers, peptides offer the advantage of forming hydrogels by exploiting physical cross-linking phenomena, avoiding the use of toxic molecules required to prompt the connection between the polymer chains and, also, extreme pH and temperature conditions. Moreover, the chemical and mechanical properties of the peptide-based scaffolds can be easily tuned by intervening on the primary sequence, making it possible to punctually modulate the affinity for the cargo, together with the rigidity needed to reach the best performances. In this work, two peptide-based hydrogels loaded with the CEST agent iopamidol have been prepared, characterized, and tested as potential systems for CEST-MRI imaging. Hydrogels based on the cationic peptides Ac-K1 and Ac-K2 were able to encapsulate a high amount of iopamidol to ensure excellent detection sensitivity at physiological pH. Due to their injectability and their ability to retain *in vitro* the imaging probe, these hydrogels can be considered promising systems to design *in vivo* MRI procedures for monitoring the release of bioactive compounds from the gel or to act as pH sensors by exploiting the well-established ability of iopamidol to generate a pH-sensitive and concentration independent CEST-MRI contrast. Both Ac-K1 and Ac-K2 hydrogels are highly biocompatible and no cytotoxicity or adverse effect was observed in mice. Work needs to be done to improve and modulate the *in vivo* stability of such hydrogels. In conclusion, to the best of our knowledge, this work demonstrates for the first time that peptide-based hydrogel scaffolds can be successfully used for designing and developing new biomedical imaging procedures based on CEST-MRI detection.

Author contributions

Conceptualization, A. A., E. T., E. D. G.; methodology, E. R., E. D. G. G. F., A. A., E. T.; software, E. D. G.; investigation, E. R., E. D. G., G. F., C. D., E. G.; resources, A. A., E. T.; data curation, E. R., E. D. G., G. F.; writing—original draft preparation, E. R., E. D. G., A. A., E. T.; writing—review and editing, E. R., E. D. G., G. F., A. A., E. T.; supervision, A. A, E. T. All authors have read and agreed to the published version of the manuscript.

Conflicts of interest

There are no conflicts to declare.

Acknowledgements

The work has received funding from the Italian Ministry of Research (PRIN project 2017 ''Rationally designed nanogels embedding paramagnetic ions as MRI probes'', A. A., E. T.). The authors acknowledge the Italian Ministry of Research for

FOE contribution to the EuroBioImaging MultiModal Molecular Imaging Italian Node (www.mmmi.unito.it). This research was performed in the framework of COST Action AC15209 (EURELAX). The work has received funding from the PNRR M4C2-Investimento 1.4-CN00000041 "Finanziato dall'Unione Europea-NextGenerationEU" (G.F.).

Notes and references

1 T. Bäuerle, M. Saake and M. Uder, *RoeFo, Fortschr. Geb. Roentgenstr. Nuklearmed.*, 2021, **193**(9), 1010–1018.
2 G. Ferrauto, S. Aime, M. T. McMahon, J. R. Morrow, E. M. Snyder, A. Li and R. Bartha in *Contrast agents for MRI: Experimental methods*, ed. V. C. Pierre and M. J. Allen, The Royal Society of Chemistry, 2018, pp. 243–317.
3 D. L. Longo, F. Michelotti, L. Consolino, P. Bardini, G. Digilio, G. Xiao, P. Z. Sun and S. Aime, *Invest. Radiol.*, 2016, **51**, 155–162.
4 S. Aime, L. Calabi, L. Biondi, M. De Miranda, S. Ghelli, L. Paleari, C. Rebaudengo and E. Terreno, *Magn. Reson. Med.*, 2005, **53**, 830–834.
5 B. F. Moon, K. M. Jones, L. Q. Chen, P. Liu, E. A. Randtke, C. M. Howison and M. D. Pagel, *Contrast Media Mol. Imaging*, 2015, **10**, 446–455.
6 H. Kim, Y. Wu, D. Villano, D. L. Longo, M. T. McMahon and P. Z. Sun, *Methods Mol. Biol.*, 2021, **2216**, 667–688.
7 Q. Tao, P. Yi, Z. Cai, Z. Chen, Z. Deng, R. Liu and Y. Feng, *Quant. Imaging Med. Surg.*, 2022, **12**, 3889–3902.
8 J. Esmaeili, A. Barati, J. Ai, V. T. Nooshabadi and Z. Mirzaei, *RSC Adv.*, 2021, **11**, 10646–10669.
9 J. Zheng, X. Song, Z. Yang, C. Yin, W. Luo, C. Yin, Y. Ni, Y. Wang and Y. Zhang, *J. Controlled Release*, 2022, **350**, 898–921.
10 J. L. Drury and D. J. Mooney, *Biomaterials*, 2003, **24**, 4337–4351.
11 S. Kuddannaya, W. Zhu and J. W. M. Bulte, *Methods Mol. Biol.*, 2022, **2394**, 743–765.
12 W. Zhu, C. Chu, S. Kuddannaya, Y. Yuan, P. Walczak, A. Singh, X. Song and J. W. M. Bulte, *Adv. Funct. Mater.*, 2019, **29**, 1903753.
13 L. L. Lock, Y. Li, X. Mao, H. Chen, V. Staedtke, R. Bai, W. Ma, R. Lin, Y. Li, G. Liu and H. Cui, *ACS Nano*, 2017, **11**, 797–805.
14 T. Jin, F. J. Nicholls, W. R. Crum, H. Ghuman, S. F. Badylak and M. Modo, *Biomaterials*, 2017, **113**, 176–190.
15 S. M. Dorsey, M. Haris, A. Singh, W. R. T. Witschey, C. B. Rodell, F. Kogan, R. Reddy and J. A. Burdick, *ACS Biomater. Sci. Eng.*, 2015, **1**, 227–237.
16 Y. Liang, A. Bar-Shir, X. Song, A. A. Gilad, P. Walczak and J. W. M. Bulte, *Biomaterials*, 2015, **42**, 144–150.
17 X. Han, J. Huang, A. K. W. To, J. H. C. Lai, P. Xiao, E. X. Wu, J. Xu and K. W. Y. Chan, *Theranostics*, 2020, **10**, 2215–2228.
18 S. Mondal, S. Das and A. K. Nandi, *Soft Matter*, 2020, **16**, 1404–1454.
19 C. Diaferia, M. Ghosh, T. Sibillano, E. Gallo, M. Stornaiuolo, C. Giannini, G. Morelli, L. Adler-Abramovich and A. Accardo, *Soft Matter*, 2019, **15**(3), 487–496.
20 J. Li, R. Xing, S. Bai and X. Yan, *Soft Matter*, 2019, **15**, 1704–1715.
21 R. M. Gouveia, V. Castelletto, S. G. Alcock, I. W. Hamley and C. J. Connon, *J. Mater. Chem. B*, 2013, **1**, 6157–6169.
22 C. Diaferia, E. Rosa, A. Accardo and G. Morelli, *J. Pept. Sci.*, 2022, **28**(1), e3301.
23 Y. Loo, A. Lakshmanan, M. Ni, L. L. Toh, S. Wang and C. A. E. Hauser, *Nano Lett.*, 2015, **15**, 6919–6925.
24 E. Rosa, F. Carniato, L. Tei, C. Diaferia, G. Morelli, M. Botta and A. Accardo, *Pharmaceuticals*, 2022, **15**, 1572.
25 C. Diaferia, E. Rosa, E. Gallo, G. Smaldone, M. Stornaiuolo, G. Morelli and A. Accardo, *Biomedicines*, 2021, **9**, 678.
26 P. Z. Sun, D. L. Longo, W. Hu, G. Xiao and R. Wu, *Phys. Med. Biol.*, 2014, **59**(16), 4493–4504.
27 D. L. Longo, W. Dastrù, G. Digilio, J. Keupp, S. Langereis, S. Lanzardo, S. Prestigio, O. Steinbach, E. Terreno, F. Uggeri and S. Aime, *Magn. Reason. Med.*, 2011, **65**(1), 202–211.
28 S. H. Yalkowsky, Y. He and P. Jain, *Handbook of Aqueous Solubility Data*, CRC Press, Boca Raton, FL, 2nd edn, 2010, 1141.